OKU Fen Bilimleri Enstitüsü Dergisi
8(4): 1780-1794, 2025

OKU Journal of The Institute of Science and Technology, 8(4): 1780-1794, 2025

Osmaniye Korkut Ata Üniversitesi Fen Bilimleri Enstitüsü Dergisi

Osmaniye Korkut Ata University Journal of The Institute of Science and Technology

n-In_2S_3/p-Si Tabanlı Heteroeklem Fotodedektörlerin Üretimi ve Karakterizasyonu

Esra ASLAN[1*]

[1]Harran Üniversitesi, Fen Edebiyat Fakültesi, Fizik Bölümü, 63300, Şanlıurfa

[1]https://orcid.org/0000-0002-3987-1570
*Sorumlu yazar: esrapalaliaslan@gmail.com

Araştırma Makalesi

Makale Tarihçesi:
Geliş tarihi: 16.01.2025
Kabul tarihi: 04.05.2025
Online Yayınlanma:16.09.2025

Anahtar Kelimeler:
Fotodedektör
Heteroeklem
In_2S_3
İnce film
Silisyum

ÖZ

In_2S_3, uygun yasak bant aralığı nedeniyle optoelektronik uygulamalarda tercih edilen bir yarıiletkendir. Bu çalışmada, In_2S_3 filmler kimyasal çözelti yöntemiyle farklı S/In molar oranlarda hazırlanmış ve yapısal, morfolojik ve optiksel özellikleri incelenmiştir. Ayrıca, p tipi silisyum altlıklar üzerine In_2S_3 ince filmler spin kaplama tekniği ile kaplanarak n-In_2S_3/p-Si yapısında heteroeklem fotodedektör cihazlar hazırlanmıştır. X-ışını kırınımı sonuçlarına göre tüm filmler tetragonal yapıda kristalleşmektedirler. Taramalı elektron mikroskobu görüntüleri filmlerin tanecikli yapıda olduğunu göstermektedir. Filmlerin yasak bant aralıkları 2.84 eV ile 2.94 eV aralığında S/In oranına bağlı olarak değişiklik göstermektedir. Karanlık ortamda yapılan ölçümlere göre cihazlar pn eklem diyot karaktersitik yapıdadırlar. Görünür ışık altında yapılan ölçümler ise cihazların ışığa tepki verdiğini göstermektedir. 5 mW/cm^2 görünür ışık altında cihazların fotohassasiyetleri 3396 gibi yüksek bir değere ulaşmaktadır. Maksimum fotoyanıt ve spesifik tespit ise 9×10^{-3} A/W ve 6.2×10^{10} Jones olarak kaydedilmiştir. Bununla birlikte, bu cihazların yükselme ve bozulma süreleri 1 saniyenin altında değerlere sahiptir. S/In oranı ayarlanarak cihazların karanlık akımları 3.7×10^{-10} A değerine kadar düşürülmüştür. Bu kadar düşük karanlık akım da cihazların spesifik tespit değerlerini 6.2×10^{10} Jones değerine kadar yükseltmiştir. Bu çalışma sonuçları In_2S_3 yarıiletkenin p tipi silisyum ile pn eklem yapı oluşturmak için son derece uygun bir malzeme olduğunu göstermektedir. Ayrıca In_2S_3 yarıiletkeni hazırlanırken çözeltideki S/In oranındaki değişim filmlerin hem fiziksel özelliklerini hemde cihazların parametrelerini önemli ölçüde etkilemektedir.

Fabrication and Characterization of n-In_2S_3/p-Si Based Heterojunction Photodetectors

Research Article

Article History:
Received: 16.01.2025
Accepted: 04.05.2025
Published online:16.09.2025

Keywords:
Heterojunction
In_2S_3
Photodetector
Silicon
Thin film

ABSTRACT

In_2S_3 is a preferred semiconductor in optoelectronic applications due to its favorable bandgap. In this study, In_2S_3 films were prepared at different S/In molar ratios by chemical solution method and their structural, morphological and optical properties were examined. In addition, heterojunction photodetector devices with n- In_2S_3/p-Si structure were prepared by coating In_2S_3 thin films on p-type silicon substrates with the spin coating technique. According to X-ray diffraction results, all films crystallize in a tetragonal structure. Scanning electron microscope images show that the films have a granular structure. The band gaps of the films vary between 2.84 eV and 2.94 eV depending on the S/In ratio. According to the measurements made in the dark environment, the devices have a *pn* junction diode characteristic structure. Measurements made under visible light show that the devices respond to light. Under 5 mW/cm^2 visible light, the photosensitivity of the devices reaches a high value of 3396. The maximum photoresponsivity and specific detectivity were recorded as 9×10^{-3} A/W, and 6.2×10^{10} Jones.

Moreover, these devices have rise and decay times of less than 1 second. By adjusting the S/In ratio, the dark current of the devices was reduced to 3.7×10^{-10} A. This low dark current also increased the specific detectivity values of the devices up to 6.2×10^{10} Jones. The results of this study clearly show that, In_2S_3 semiconductor is a highly compatible material for forming pn junction structure with p-type silicon. In addition, while preparing the In_2S_3 semiconductor, the change in the S/In ratio in the solution significantly affects both the physical properties of the films and the parameters of the devices.

To Cite: Aslan E. Fabrication and Characterization of n-In_2S_3/p-Si Based Heterojunction Photodetectors. Osmaniye Korkut Ata Üniversitesi Fen Bilimleri Enstitüsü Dergisi 2025; 8(4): 1780-1794.

1. Introduction

Semiconductor materials are the cornerstone of optoelectronic applications. Their interaction with light has led to the frequent use of such materials in applications such as solar cells, photocatalytics and photodetectors (Ahmad et al., 2023; Aslan et al., 2024). Photodetectors that detect light can generally be classified into two categories according to their working principles: metal-semiconductor-metal (MSM) and pn junction type. On the other hand, MSM-type photodetectors are divided into two subcategories: ohmic contact and Schtokky contact. Ohmic contact and Schottky contact structure can be determined according to the work functions of metals and semiconductors. In ohmic contact photodetectors, when light is absorbed by the semiconductor, an electron-hole pair is formed. Under an external voltage, this pair separates from each other and creates photocurrent. This external voltage usually varies between 5 and 20 V (Kumar and Kumar, 2019; Qin et al., 2019). In such devices, the need for these high external voltage values to observe the change in current under light is considered a disadvantage. Besides that, in Schottky contact and pn junction-type photodetectors, the electron-hole pairs produced by photon absorption are separated from each other due to the potential difference in the junction region without an external voltage, creating photocurrent. Therefore, this type of photodetectors is more advantageous as they provide their own energy. Such devices are also called self-powered devices. Such devices are needed, especially in places where energy is difficult to deliver. Therefore, the development of such devices is also essential. Studies on self-powered photodetectors are increasing rapidly. For example, perovskite-based photodetectors are attracting much attention (Wang et al., 2022). However, although perovskite structures have excellent properties, there are serious problems with their instability. Therefore, alternative heterostructures need to be investigated. Silicon semiconductor, with its 1.12 eV bandgap, forms the basis of all electronic technology. It is possible to produce p and n-type silicon depending on the doping type. Junctions obtained with p-type silicon and n-type silicon are called homojunctions. However, it is also possible to obtain a pn junction with two different semiconductors. Such structures are called heterojunctions. Heterojunction structures have been obtained by coating many different semiconductors on p-type silicon as a photodetector. Examples include p-Si/n-ZnO, p-Si/n-ZnS, p-Si/n-TiO_2 and p-Si/n-CdS heterojunctions (Al-Ani et al., 2006; Zhang et al., 2020; Agrohiya et al., 2022; Moger and Mahesha, 2023). Generally, wide band gap semiconductors are preferred for such structures. For instance, the band gaps of ZnO, ZnS, TiO_2 and CdS are 3.3, 3.8, 3.6 and 2.6 eV,

respectively (Hankare et al., 2009; Wei et al., 2013; Khan et al., 2017; Muchuweni et al., 2017). CdS is an excellent semiconductor for both photodetectors and solar cells. However, its use is restricted because it contains heavy metals that are harmful to the environment. Therefore, scientists have researched materials that could be alternatives to this material. One of the materials investigated is In_2S_3. This material has attracted attention due to its suitable band gap and high sensitivity to light. It has been widely researched as an n-type material, especially in solar cells (Robin and Rahaman, 2016). In_2S_3 semiconductor is a sulfur compound and the amount of sulfur in its structure can affect many of its physical properties, especially the band gap. In this study, heterojunction photodetectors were prepared by coating n-type In_2S_3 semiconductor on p-type silicon by chemical solution method. The sulfur ratio in the In_2S_3 material was changed depending on the molar ratio of the sulfur-containing chemical added to the solution. Structural, morphological, optical and photodetector properties of films prepared with solutions of different molar ratios were examined in detail. According to the results, the amount of sulfur in the solution significantly affects both the physical properties and photodetector parameters of In_2S_3.

2. Material and Methods

2.1. Preparation of In_2S_3 solutions and thin films

Indium (III) chloride hydrate ($InCl_3 \cdot \times H_2O$), thiourea (CH_4N_2S), 2-methoxyethanol ($C_3H_8O_2$), and ethanolamine (C_2H_7NO) chemicals were used for the preparation of In_2S_3 solutions and thin films. After dissolving 0.8847 g of indium (III) chloride hydrate in 17 ml of 2-methoxyethanol at room temperature, 0.1523 g of thiourea was added to this solution. The S/In ratio in this solution is 2/4. Finally, ~ 0.1 ml of ethanolamine base was added to the solution after mixing on a magnetic stirrer for 30 minutes. After 24 hours of mixing, transparent light yellow solutions were obtained. Along with this solution, three more solutions with S/In ratios of 6/4, 10/4 and 14/4 were prepared. These solutions were prepared similarly. The pH value of all solutions was measured to be ~ 4.7. Using these solutions, coated films were formed 7 times on glass substrates by dipping method at 300 ^oC. These films were then annealed in a vacuum environment at 350 ^oC for 30 minutes.

2.2. Preparation of p-Si/n-In_2S_3/Ag photodetectors

Commercially available p-type and (100) oriented silicon substrates were used. The conventional hydrofluoric acid cleaning process was applied to remove the native SiO_2 layer formed on Silicon (Zhang et al., 2020; Moger and Mahesha, 2023). After the cleaning process of the substrates, carbon paste was applied to the underside (unpolished side), and kept at 150 ^oC for 5 minutes on a hot plate. Then, silver paste was applied on the carbon layer, and the same heat treatment was repeated. In_2S_3 films were coated on the polished surface of a silicon wafer using the spin coating technique at 3000 rpm. In_2S_3 films were coated 5 times, and kept at 300 ^oC for 3 minutes after each coating. Finally, silver contacts were formed by the thermal evaporation method using a mask on the In_2S_3 layer. Figure 1 shows the schematic structure of the prepared photodetectors.

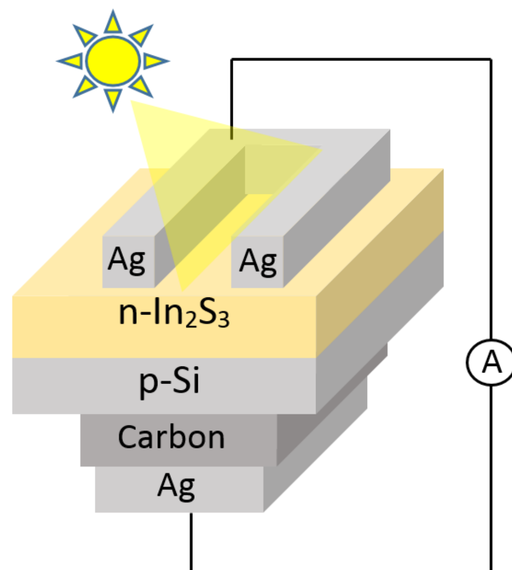

Figure 1. Schematic representation of the prepared self-powered photodetectors

2.3. Characterization

X-ray diffraction (XRD), scanning electron microscopy (SEM) and UV-Vis spectrometry methods were used for structural, morphological and optical measurements, respectively. A Keithley 2400 source-meter and white light-emitting LED were used for the characterization of photodetectors. The intensity of the light was adjusted to 5 mW/cm^2 using a Newport power meter. All measurements were carried out at room temperature, and in a closed box.

3. Results and Discussion

In order to determine the crystal structures of In_2S_3 samples, measurements were made with the XRD device, with 2θ angles between 10 and 70°, in steps of 0.03°. Figure 2 shows the XRD spectra of all samples. The peaks appearing at 14.61°, 27.65°, 33.39°, 43.79°, and 47.82° belong to the (103), (213), (220), (309), and (400) planes of In_2S_3, which has a tetragonal crystal structure, respectively (Lin et al., 2014). In films with a S/In ratio of 2/4, XRD peaks belonging to the In_2O_3 phase appeared along with the In_2S_3 phase (see Fig. 2a). As seen in the figure, the peak appearing at ~ 31 degrees belongs to In_2O_3 with the Miller indice of (222) (Wang et al., 2024). This may be due to the low sulfur content in these films. When there is not enough sulfur in the structure, indium metal may tends to oxidize. This is an expected result. However, as the sulfur content increases, the intensity of the XRD peak of (222) crystalline plane decreases significantly. This result shows how the sulfur content in the films affects the formation of different phases such as In_2O_3. On the other hand, according to XRD results, the In_2S_3 phase was formed in all films.

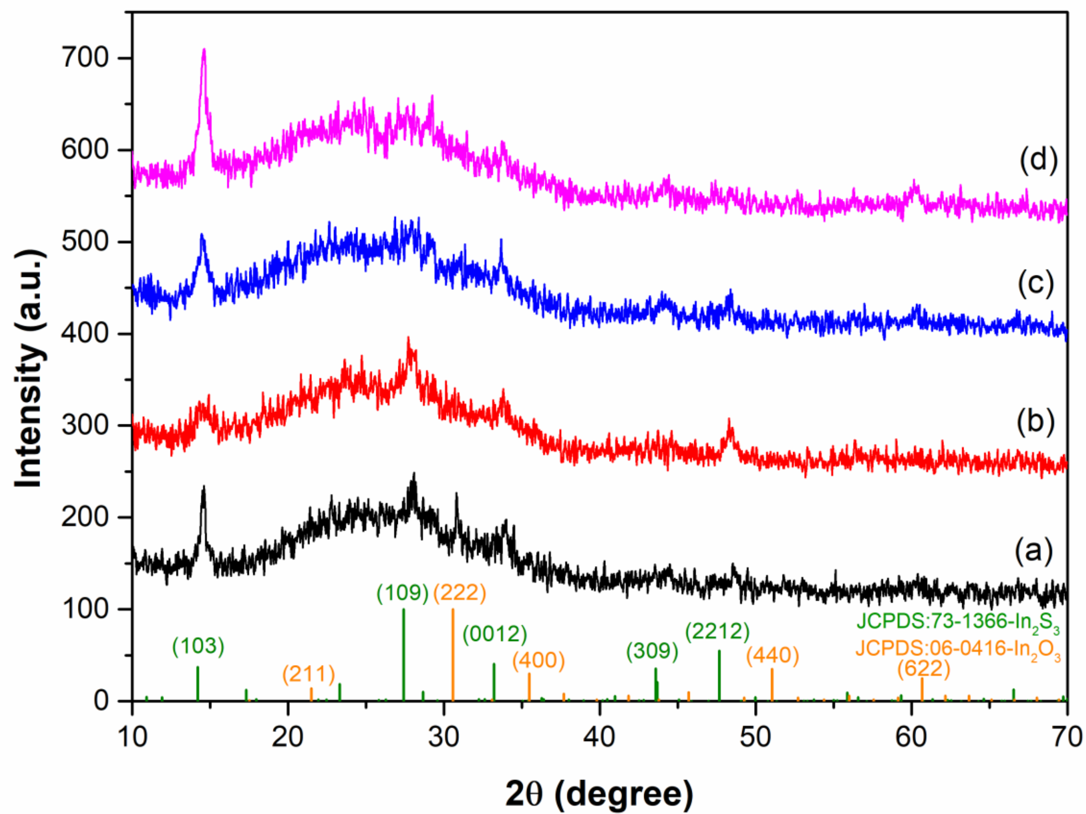

Figure 2. XRD patterns of samples with S/In ratio of (a) 2/4, (b) 6/4, (c) 10/4, (d) 14/4

The crystallite size of the samples was also calculated using the Sherrer relation below.

$$D = \frac{0.9\lambda}{\beta\cos(\theta)} \tag{1}$$

In this equation, λ represents the X-ray beam wavelength (1.54 Å), D is the crystallite size, β is the full width at half maximum (FWHM), θ is the Bragg angle, and 0.9 is the shape factor (Bchiri et al., (2021). The crystallite sizes for the intense (109) XRD peak were calculated. FWHM and crystallite sizes of films with S/In ratios of 2/4, 6/4, 10/4, and 14/4 are determined as (0.4171, 18.9 nm), (0.9799, 8.1 nm), and (0.8326, 9.5 nm), and (0.6106, 13.1 nm), respectively. According to the results, the crystallite sizes of the films vary between 8.1 and 18.9 nm depending on the S/In ratio. As the sulfur content in the solution increases, the crystallite size first decreases and then increases again. SEM images were used to examine the effects of the sulfur ratio on the surface structures of the films. Figure 3 shows the SEM results of the films prepared by changing the sulfur ratios.

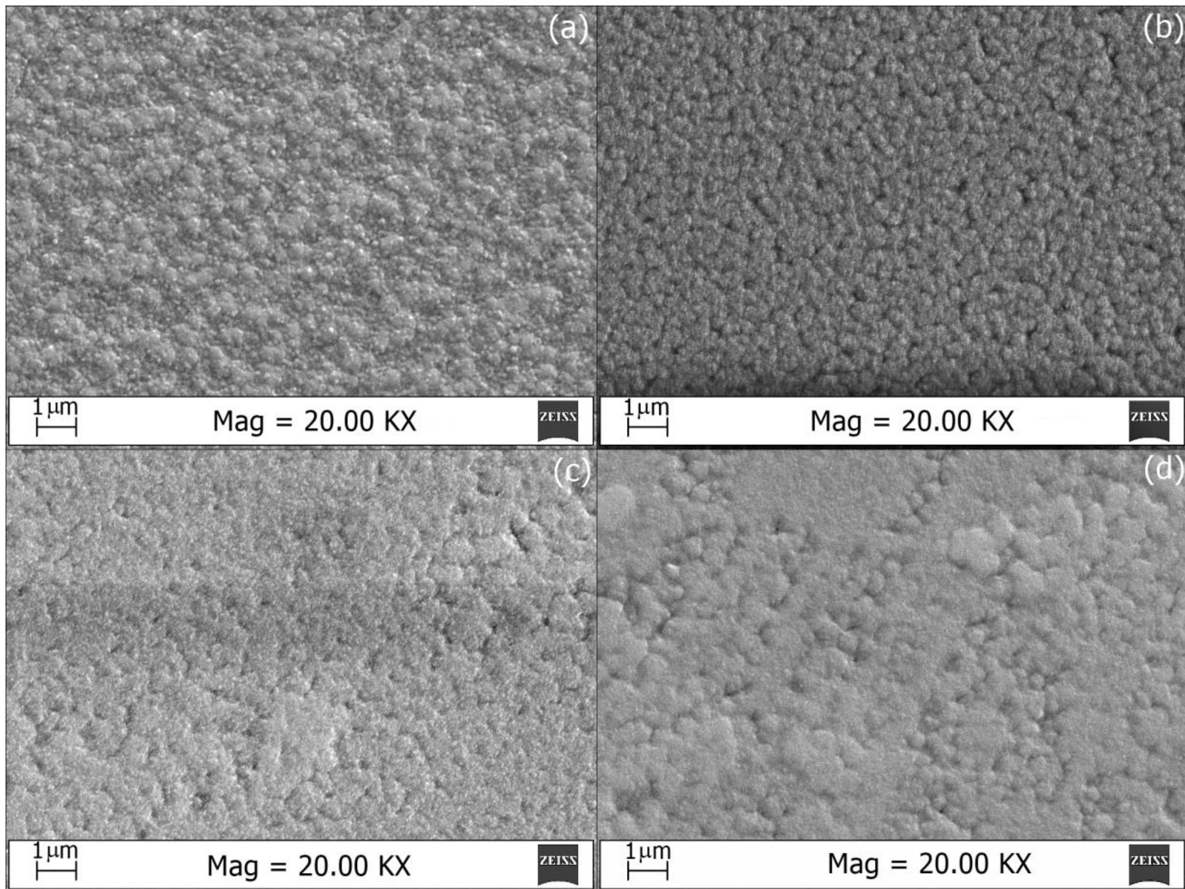

Figure 3. SEM images of samples with S/In ratio of (a) 2/4, (b) 6/4, (c) 10/4, (d) 14/4

According to the SEM images, the surfaces of the films have a granular structure. As the sulfur content increases, the surface structures of the films change. It has been observed in the literature that the amount of sulfur in other sulfur compounds changes the surface structure of the films. For example, SEM images of CZTS films prepared by the sol–gel method showed that a higher amount of sulfur content resulted in a compact, and smooth surface compared to samples sulfurized at lower sulfur concentrations (Ashfaq et al., 2021). A similar result was also observed for $CuInS_2$ thin films. As the sulfuration time increased, a denser structure was observed (Ligang et al., 2015). Therefore, the results obtained are compatible with the literature. In order to determine the optical properties of the prepared thin films, optical transmittance spectra were obtained with UV-Vis spectrometry in the wavelength range of 200 to 1100 nm. Figure 4 shows the optical transmittance spectra of all samples.

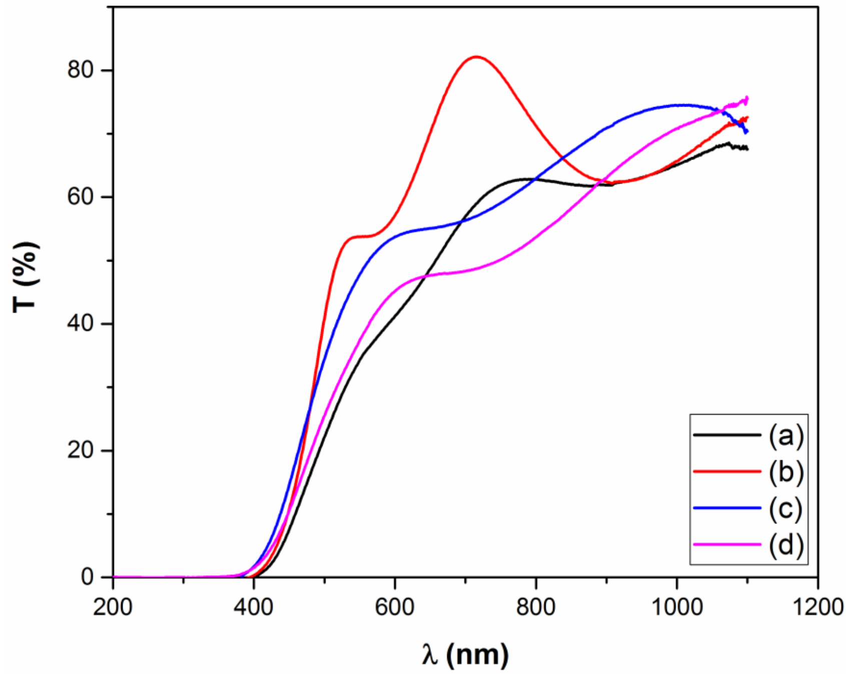

Figure 4. Transmittance spectrum of samples with S/In ratio of (a) 2/4, (b) 6/4, (c) 10/4, (d) 14/4

According to the spectra in Figure 4, it is observed that the optical transmittance over the 700 nm wavelength is 60 % on average in films with an S/In ratio of 2/4. When the S/In ratio is 6/4, there is a significant increase in optical transmittance in the visible region. There are optical studies in the literature based on sulfur content or sulfurization time. Generally, as the sulfurization time increases in sulfur compounds, the optical transmittance of the films also increases. For instance, when the sulfurization time in the SnS semiconductor prepared by the magnetron sputtering method is increased from 10 minutes to 60 minutes, the optical transmittance in the visible region increases from 30 % to 50 % (Gurubhaskar et al., 2018). However, when the S/In ratio exceeds a specific value, the optical transmittance decreases again (Fig.4d). One of the most important information that can be obtained from the optical spectrum is the α absorption coefficient of the films. The absorption coefficient can be determined by the following relation (Chapi et al., 2020).

$$\alpha = \frac{2.303\ A}{d} \tag{2}$$

where A is the absorbance and d is the film thickness. Measurements made with an ellipsometer show that the thickness of the films is approximately 300 nm. On the other hand, it is also possible to determine the forbidden band gaps of films using the Tauc relation below, using the α absorption coefficient (Chapi et al., 2020).

$$\alpha h v = B(hv - E_g)^n \tag{3}$$

In this relation, B is a constant, h is the Planck constant, α is the absorption coefficient, v is the frequency, E_g is the forbidden band gap and $n = ½$ for direct allowed transitions. The slope of the graph of $(\alpha hv)^2$ versus hv in this relation corresponds to the forbidden band gap. Figure 5 shows the slopes of the graph drawn according to this relation.

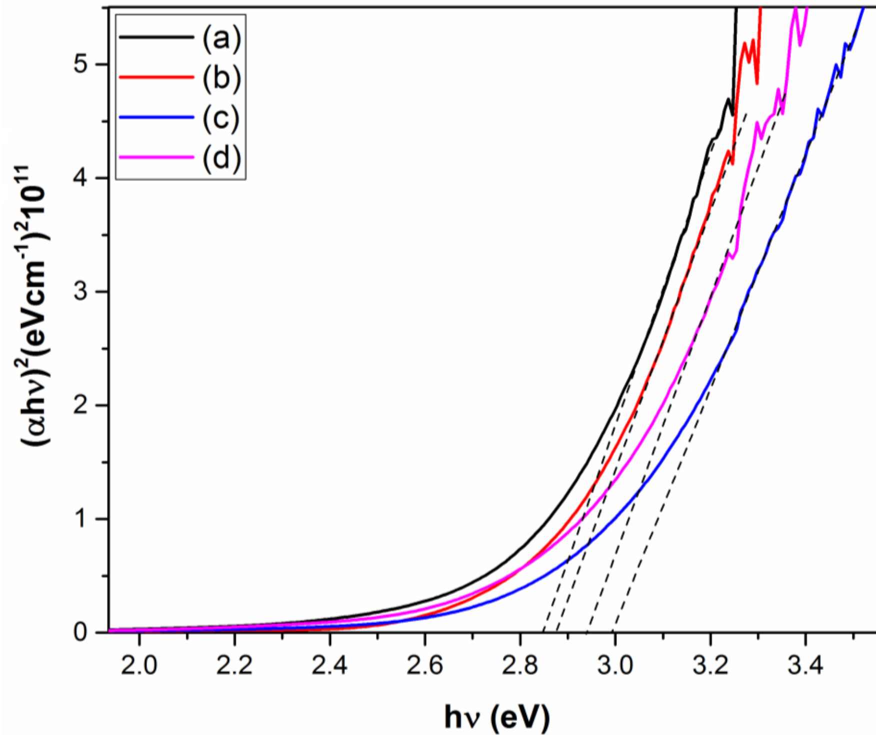

Figure 5. Forbidden band gaps of samples with S/In ratio of (a) 2/4, (b) 6/4, (c) 10/4, (d) 14/4

According to the slopes of the graphs in the figure, the forbidden band gaps of films with S/In ratios of 2/4, 6/4, 10/4, and 14/4 are determined as 2.84, 2.88, 2.99, and 2.94 eV, respectively. It has been observed that the forbidden band gap increases with a certain sulfur content and then decreases again. The widening of the forbidden band gap with increasing sulfur content in sulfur compounds has been recorded in many studies. For example, in the research conducted by Ebrahimi et al. (2017), depending on the Zn/S ratio in ZnS films prepared by the spray pyrolysis method, they showed that, the band gap increased from 3.43 to 3.72 eV as the sulfur ratio increased. Another example of sulfur compounds is the Sb_2S_3 semiconductor. In Sb_2S_3 films prepared by magnetron sputtering method, it was observed that by increasing the sulfurization time, the band gap increased from 1.61 to 1.69 eV and then decreased again (Uc-Canché et al., 2024). Therefore, the change observed in the forbidden band gap depending on the sulfur content in this study is well compatible with the literature. In order to examine the effect of the prepared films on photodetectors, devices with Ag/C/p-Si/n-In_2S_3/Ag structure were prepared. Here, it has been observed that the contacts obtained by first applying carbon paste and then silver on p-type silicon are ohmic. Semi-logarithmic IV curves recorded in the dark environment of the devices prepared by coating In_2S_3 films on the polished surface of silicon are given in Figure 6.

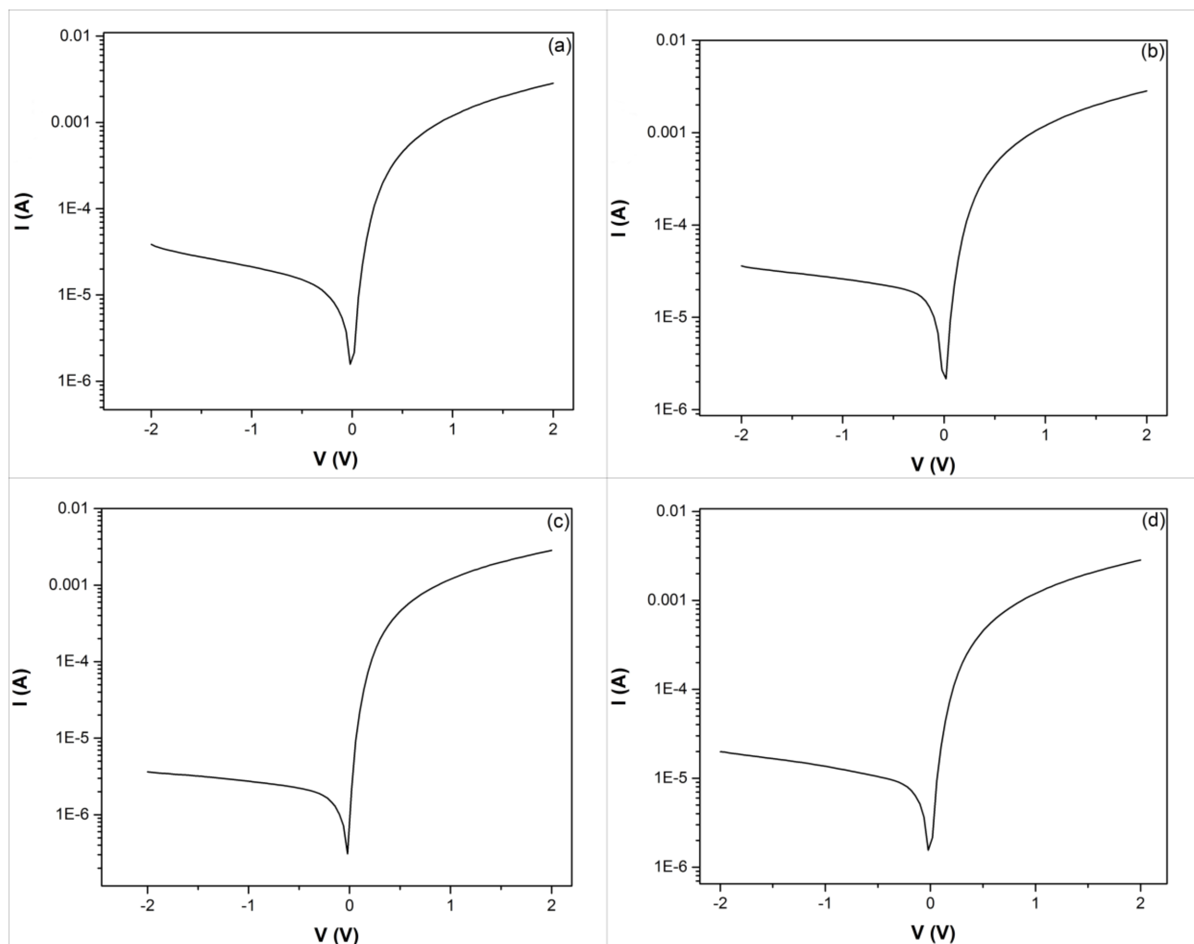

Figure 6. Semi-logarithmic IV curves of devices with S/In ratio of (a) 2/4, (b) 6/4, (c) 10/4, (d) 14/4

As seen in Figure 6, all devices show diode characteristics. According to this result, In_2S_3 films form a pn junction structure with p-type silicon. In order to observe the reactions of these devices under light, an LED source emitting white light of 5 mW/cm^2 was used. In Figure 7, the change graph of the current of the prepared photodetectors depending on time in the dark, and light environment at zero external voltage is given.

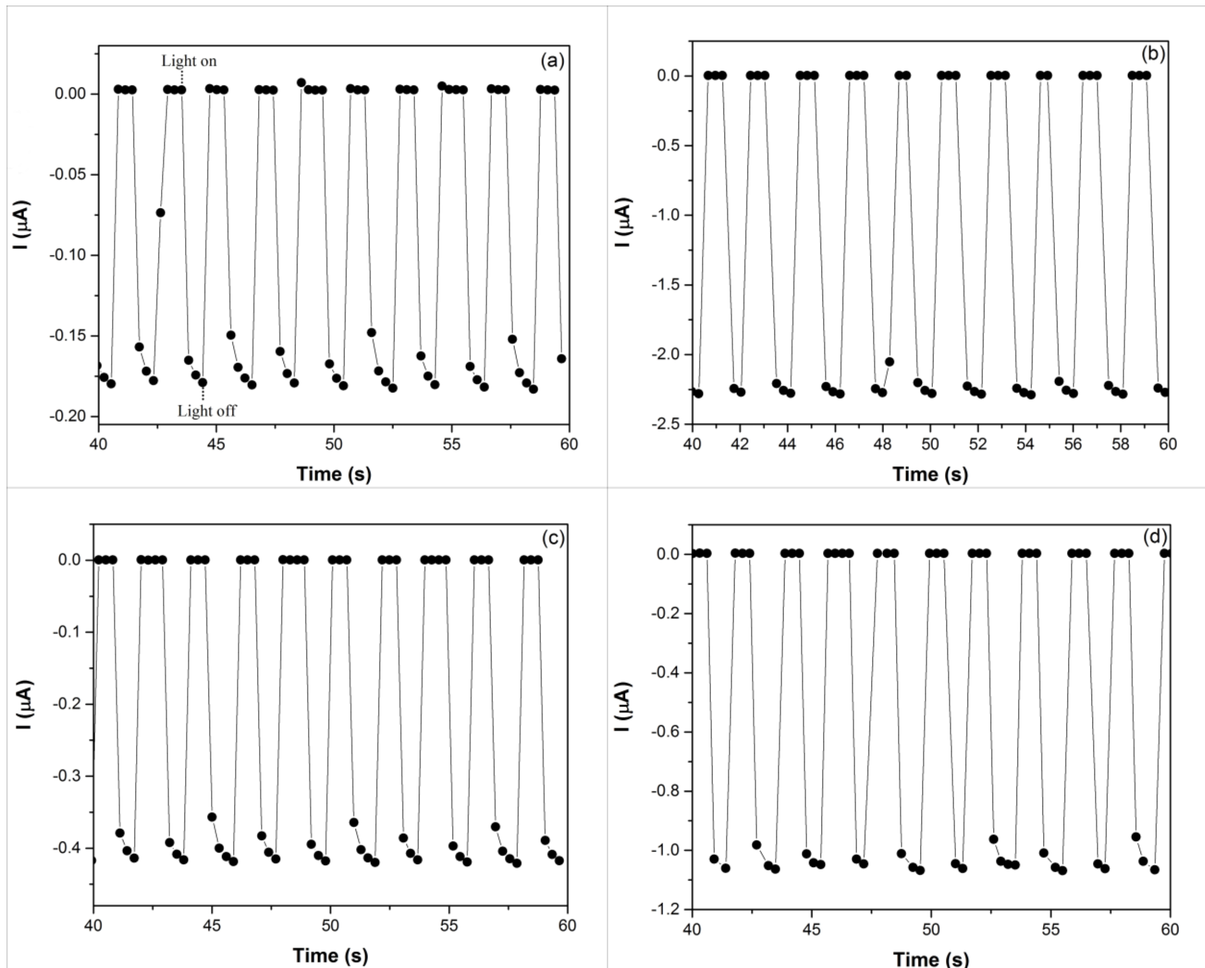

Figure 7. Current-time graph of devices with S/In ratio of (a) 2/4, (b) 6/4, (c) 10/4, (d) 14/4

As seen in the figure, when the light is turned on, current passes through the circuit quickly and when the light is turned off, it quickly returns to its previous value. The is because that light falls on the *pn* junction region formed between the p-Si semiconductor and the n-In_2S_3 semiconductor and excites the electrons in that region and turns them into photocurrent. To scale this rate of change in current, rise and decay time parameters are measured in photodetectors. When the light is turned on, the rise time of a photodetector is the amount of time it takes for the photocurrent to increase from 10% to 90%. Alternatively, decay time is the amount of time it takes for the current to drop from 90% to 10% when the light is switched off. (Kumar et al., 2019). Figure 8 shows the time parameters of photodetectors prepared with films with a S/In ratio of 2/4. As seen in Figure 8, the rise and decay times for these devices were recorded as 0.25 and 0.23 s, respectively. These response times are quite short for a photodetector. It means that the device responds quickly to light. The time parameters of other devices with S/In ratios of 6/4, 10/4 and 14/4 are calculated as (0.41 s, 0.30 s), (0.24 s, 0.22 s), and (0.24 s, 0.39 s), respectively. The time parameters of all devices are approximately in the same order.

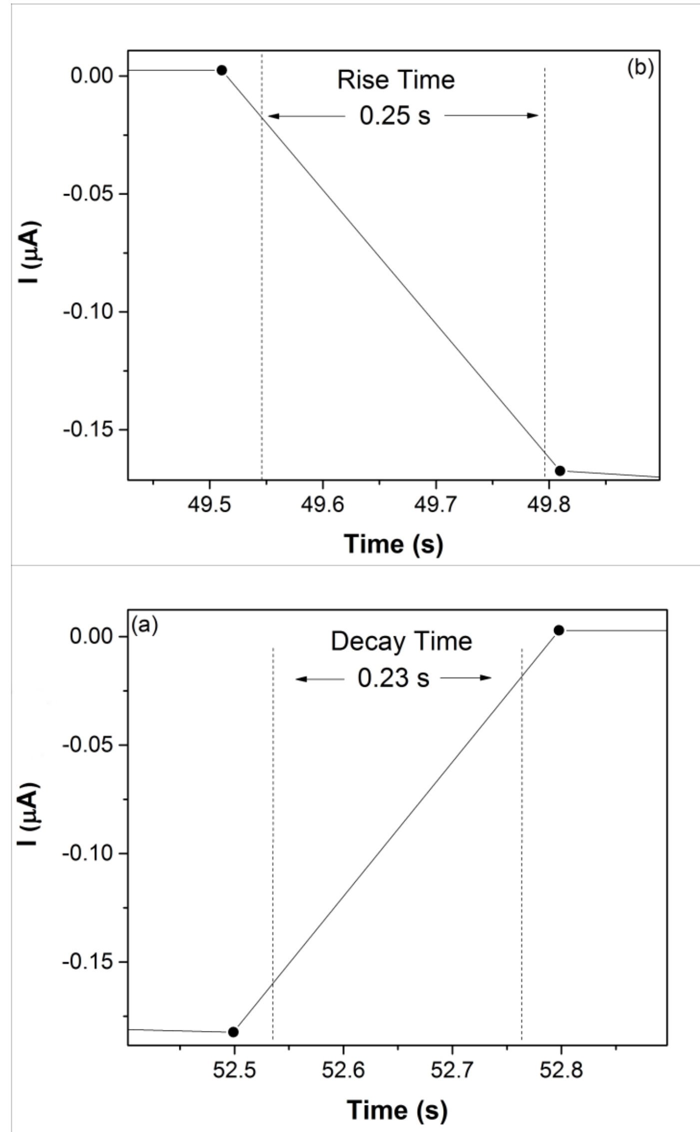

Figure 8. (a) Rise and (b) decay times of device with S/In ratio of 2/4

Kumar and his colleagues (2019) recorded rise and decay times of 3.75 and 3.68 seconds under visible light in MSM type photodetectors obtained with In_2S_3 films prepared by thermal evaporation method. Therefore, the values obtained in this study are quite low compared to those of similar studies in the literature. On the other hand, the dark currents of the prepared devices are determined as 2.7×10^{-9} A, 3.5×10^{-9} A, 3.7×10^{-10} A, and 3.4×10^{-9} A, respectively. These dark current values are also quite low. It is preferred for photodetectors to have low dark current. The maximum current values that can be obtained from the devices when the light is turned on are 1.8×10^{-7} A, 2.3×10^{-6} A, 4.0×10^{-7} A, and 1.0×10^{-6} A, respectively. It can be seen that the current changes significantly under light for all devices. The following formulas are used to calculate the photodetector's photosensitivity (Aslan et al., 2024).

$$I_P = I_I - I_D \quad (4)$$

$$S = \frac{I_P}{I_D} \quad (5)$$

where, S is the photosensitivity, I_p is the photo-current, I_D is the dark current, and I_l is the current under the light. For devices with S/In ratios of 2/4, 6/4, 10/4 and 14/4, photosensitivity is calculated as 177, 2296, 3996, and 293, respectively. According to these results, the S/In ratio in In_2S_3 films significantly affects the interaction of the devices with light. Maximum photosensitivity was observed in samples with an S/In ratio of 10/4. The values obtained in this study are higher than similar studies in the literature. For instance, Salam et al. (2024) observed a photosensitivity of 177 under visible light with In_2S_3-based heterojunction photodetectors prepared by spray the pyrolysis method. The photoresponsivity and specific detectivity parameters of the prepared photodetectors were calculated with the following equations (Gong et al., 2023).

$$R = \frac{I_P}{P_{in}A_o} \tag{6}$$

$$D = R\left(\frac{A_o}{2qI_D}\right)^{\frac{1}{2}} \tag{7}$$

where, R is the photoresponsivity, P_{in} is the light power density, A_o is the active surface area of the device, and q is the elementary charge. The active surface areas of the samples were measured as approximately 0.05 cm^2. The parameters calculated using these equations are given in Table 1.

Table 1. Parameters of the prepared photodetectors and comparison with other studies

Device structure	Rise time (s)	Decay time (s)	Sensitivity (S)	Responsivity (A/W)	Detectivity (Jones)	Ref.
n-In_2S_3/p-Si	0.25	0.23	177	7×10^{-4}	5.3×10^{9}	This study
n-In_2S_3/p-Si	0.41	0.30	2296	9×10^{-3}	6.0×10^{10}	This study
n-In_2S_3/p-Si	0.24	0.22	3996	2×10^{-3}	6.2×10^{10}	This study
n-In_2S_3/p-Si	0.24	0.39	293	4×10^{-3}	2.7×10^{10}	This study
n-In_2S_3/glass	0.7	0.7	2.45	3.1×10^{-3}	1.2×10^{9}	Kumar et al., (2019)
n-In_2S_3/glass	19	71	0.96	3.7×10^{-6}	7.5×10^{7}	Bchiri et al., (2021)
n-In_2S_3/F-SnO_2	9.2	17.5	177	1.2×10^{-3}	4.0×10^{10}	Salam et al., (2024)

As seen in the table, photoresponsivity values of the samples can go up to 9×10^{-3} A/W. The highest specific detectivity determination was 6.2×10^{10} Jones. As seen in the table, these results are higher than those of similar studies in the literature. The obtained time parameters also show that the devices respond to light in a short time. Especially the low decay time indicates that the electrons excited at the In_2S_3 and silicon interface are not trapped significantly in the forbidden band gap while returning to the valence band. For example, in his detailed study on CdS and CdSe semiconductor-based photoconductors, Skarman (1965) showed that the trap density in the forbidden band region significantly affects the decay time. He emphasized that, decay time could be 50 times lower in materials with low trap density. Therefore, when compared to other studies in the literature, it can be thought that, the lower time

parameters of the devices prepared in this study are due to less dense trapping centers. This is the preferred situation for photodetectors.

4. Conclusion

In this study, In_2S_3 semiconductor films were produced by the solution method. By changing the amount of chemicals in the solution, four different films were prepared depending on the S/In molar ratio. XRD results show that the films crystallize in a tetragonal crystal structure. XRD results also show that oxide phases are formed in films with low sulfur content. The band gaps of the samples vary between 2.84 and 2.94 eV. SEM images reveal that the samples have a granular structure. Furthermore, In_2S_3 films were coated on p-type silicon and heterojunction structures were obtained. The formation of pn junction structures was confirmed by IV curves. According to the results of the analysis performed under visible light, the samples create photocurrent under zero voltage. The rise and decay times of the prepared photodetectors are under 1 second. The highest photosensitivity, photoresponsivity, and specific detectivity values were recorded as 3996, 9×10^{-3} A/W, and 6.2×10^{10} Jones, respectively. As a result, In_2S_3 films are an extremely suitable semiconductor for obtaining heterojunction structures with p type silicon semiconductors. Additionally, this study shows that the S/In ratio plays a critical role in the In_2S_3 material.

Conflict of interest

The author declare that have no competing interests.

Consent for publication

The author declares that she has contributed 100% to the article.

Abbreviations

MSM: Metal-semiconductor-metal
XRD: X-ray diffraction
SEM: Scanning electron microscopy
LED: Light emitting diode
R: Photoresponsivity
D: Specific detectivity
P_{in}: Light power density
A_o : Active surface area
q: Elementary charge
S: Photosensitivity,
I_p: Photo-current,
I_D : Dark current, and
I_I : Current under light
h: Planck constant,
α: Absorption coefficient,
v: Frequency,
E_g : Forbidden band gap
A : Absorbance
d : Film thickness

References

Agrohiya S., Kumar V., Rawal I., Dahiya S., Goyal PK., Kumar V., Punia R. Fabrication of n-TiO_2/p-Si photo-diodes for self-powered fast ultraviolet photodetectors. Silicon 2022; 14: 11891–1190.

Ahmad I., Zou Y., Yan J., Liu Y., Shukrullah S., Naz MY, Hussain H., Khan QW., Khalid NR. Semiconductor photocatalysts: A critical review highlighting the various strategies to boost the photocatalytic performances for diverse applications. Advances in Colloid and Interface Science 2023; 311: 102830.

Al-Ani SKJ., Ismail RA., Al-Ta'ay HFA. Optoelectronic properties n:CdS:In/p-Si heterojunction photodetector. J Mater Sci: Mater Electron 2006; 17: 819–824.

Ashfaq A., Jacob J., Mahmood K., Mehboob K., Ikram S., Ali A., Amin N., Hussain S., Rehman U. Effect of sulfur amount during post-growth sulfurization process on the structural, morphological and thermoelectric properties of sol-gel grown quaternary chalcogenide Cu_2ZnSnS_4 thin films. Physica B: Condensed Matter 2021; 602: 412497.

Aslan E., Kaya D., Karadağ K., Harmancı U., Aslan F. Enhancing performance of SnS_2 based self-powered photodetector and photocatalyst by Na incorporation. Ceramics International 2024; 50(15): 27626-27634.

Bchiri Y., Tiss B., Bouguila N., Souissi R., Kraini M., Vázquez-Vázquez C., Khirouni K., Alaya S. Electrical investigation of sprayed In_2S_3 film. Materials Science in Semiconductor Processing 2021; 121: 105294.

Chapi S. Optical, electrical and electrochemical properties of PCL5/ITO transparent conductive films deposited by spin-coating – Materials for single-layer devices. Journal of Science: Advanced Materials and Devices 2020; 5(3): 322-329.

Ebrahimi S., Yarmand B., Naderi N. Effect of the sulfur concentration on the optical band gap energy and urbach tail of spray-deposited ZnS Films ACERP 2017; 3(4): 6-12.

Gong K., Li L., Yu W., Mu H., Yuan J., Hao R., Liu B., Mei Z., Mei L., Li H., Lin S. High detectivity and fast response avalanche photodetector based on GaSe/$PtSe_2$ p–n junction. Materials & Design 2023; 228: 111848.

Gurubhaskar M., Thota N., Raghavender M., Chandra GH, Prathap P., Subbaiah YPV. Influence of sulfurization time on two step grown SnS thin films. Vacuum 2018; 155: 318-324.

Hankare PP., Chate PA., Sathe DJ. CdS thin film: Synthesis and characterization. Solid State Sciences 2009; 11(7): 1226-1228.

Khan MI., Bhatti KA., Qindeel R., Althobaiti HS., Alonizan N. Structural, electrical and optical properties of multilayer TiO_2 thin films deposited by sol–gel spin coating. Results in Physics 2017; 7: 1437-1439.

Kumar B., Kumar MC. Indium sulfide based metal-semiconductor-metal ultraviolet-visible photodetector. Sensors and Actuators A: Physical 2019; 299: 111643.

Kumar H., Shaji B., Kumar MC. Fabrication of visible light photodetector using co-evaporated Indium Sulfide thin films. J Mater Sci:Mater Electron 2019; 30: 17986–17998.

Ligang W., Yanlai W., Wei Y., Jun Z., Jingang X. Effect of sulfurization time on the formation of $CuInS_2$ thin films. Rare Metal Materials and Engineering, 2015; 44(4): 805-807.

Lin P., Lin S., Cheng S., Ma J., Lai Y., Zhou H., Jia H. Optical and electrical properties of Ag-doped In_2S_3 thin films prepared by thermal evaporation. Advances in Materials Science and Engineering 2014; ID 370861.

Moger SN., Mahesha MG. Spectroscopic and electrical analysis of p–Si/n-ZnS_xSe_{1-x} ($0.0 \leq x \leq 1.0$) heterostructures for photodetector applications. J Mater Sci: Mater Electron 2023; 34: 958.

Muchuweni E., Sathiaraj TS., Nyakotyo H. Synthesis and characterization of zinc oxide thin films for optoelectronic applications. Heliyon 2017: 3(4): e00285.

Robin MSR., Rahaman MM. A comparative performance analysis of CdS and In_2S_3 buffer layer in CIGS solar cell, 2016 2nd International Conference on Electrical, Computer & Telecommunication Engineering (ICECTE). Rajshahi, Bangladesh 2016; 1-4, doi: 10.1109/ICECTE.2016.7879639.

Salam JA., Anand AM., Raj A., Nath A., Jayakrishnan R. Self-powered response in β-In_2S_3 thin films. Journal of Science: Advanced Materials and Devices 2024; 9(1): 100671.

Uc-Canché S., Camacho-Espinosa E., Mis-Fernández R., Loeza-Poot M., Ceh-Cih F., Peña JL. Influence of sulfurization time on Sb_2S_3 synthesis using a new graphite box design. Materials 2024; 17: 1656.

Wang H., Sun Y., Chen J., Wang F., Han R., Zhang C., Kong J., Li L., Yang JA. Review of perovskite-based photodetectors and their applications. Nanomaterials (Basel) 2022; 12(24): 4390.

Wang N., Bai Y., Zhao F., Yang X., Gu F., Wang S., Li J., Fu H., An X. Hydrothermal synthesis of La-doped In_2O_3 nanosheets-assembled microflowers for sensing n-butanol. J Mater Sci 2024; 59: 15408–15421.

Wei A., Liu J., Zhuang M., Zhao Y. Preparation and characterization of ZnS thin films prepared by chemical bath deposition. Materials Science in Semiconductor Processing 2013; 16(6): 1478-1484.

Qin Y., Long S., Dong H., He Q., Jian G., Zhang Y., Hou X., Tan P., Zhang Z., Lv H., Liu Q., Liu, M. Review of deep ultraviolet photodetector based on gallium oxide. Chinese Physics B 2019; 28(1): 018501.

Zhang Y., Hu M., Wang Z. Enhanced performances of p-Si/n-ZnO self-powered photodetector by interface state modification and pyro-phototronic effect. Nano Energy 2020; 71: 104630.